

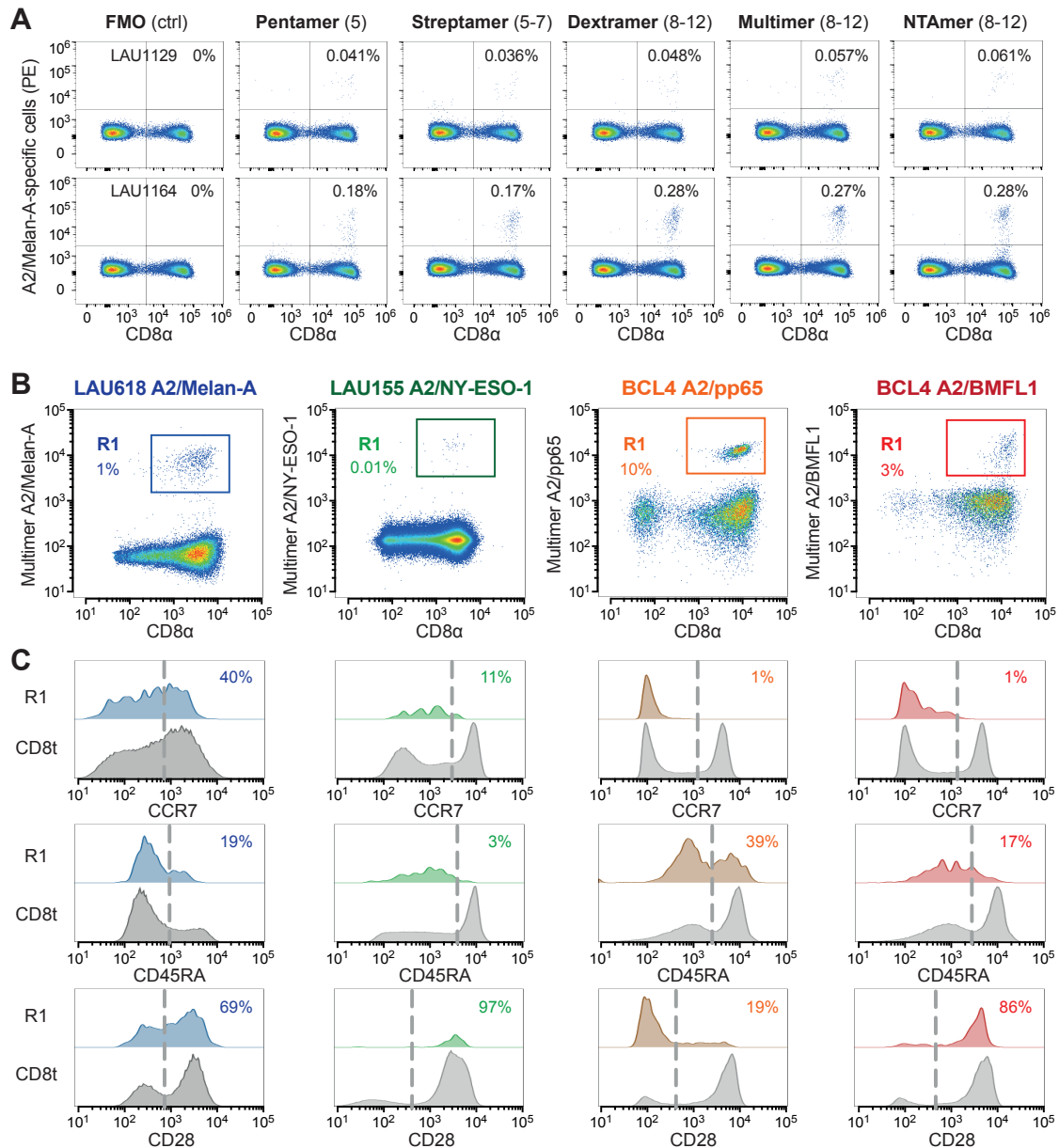
SUPPLEMENTAL MATERIALS

Supplemental Table 1. List of TCR-BV-CDR3 clonotypes and their off-rate values.

Antigenic specificity	Patient/ Donor	Clonotype	BV family	CDR3 (amino acids)	BJ	Mean koff (s-1)
A2/Melan-A	LAU618	clono 1	BV3	SPPGLSGNIQ	2.4	0.03338
		clono 2	BV3	SFQGVGTGEL	2.2	0.02622
		clono 3	BV13	SYGPLSGAGY	1.2	0.02548
		clono 4	BV13	SPGTLADTQ	2.3	0.06173
		clono 5	BV13	SAGYGQPQ	1.5	0.05155
		clono 6	BV14	RAGALQGEQ	2.7	0.10740
		clono 7	BV14	SPAALSGAYEQ	2.7	0.10100
		clono 8	BV17	SPGALNTEA	1.1	0.06438
		clono 9	BV3	SFPRWGRNYSYNEQ	na	0.03492
		clono 10	BV14	SLSAGTGVLDTQ	na	0.09449
		clono 11	BV17	SIGA--EHEQ	na	0.09964
		clono 12	BV17	SIEALQGFEA	na	0.04187
		clono 13	BV17	RWGVLNTEA	na	0.01835
A2/NY-ESO-1	LAU155	clono 1	BV1	SVATGGDTQ	2.3	0.01875
		clono 2	BV8	NSGSNEQ	2.1	0.02771
		clono 3	BV8	SLGSTEA	1.1	0.00831
		clono 4	BV8	NSGANEQ	2.1	0.02026
		clono 5	BV8	RKGPNEQ	2.1	0.03529
		clono 6	BV13	SYVGAAGEL	2.2	0.02918
		clono 7	BV13	SLTGGLNSPL	na	0.03146
		clono 8	BV1	SLATGEDTQ	na	0.01574
		clono 9	BV13	LGDGDGAYNSPL	1.6	0.03277
	LAU50	clono 10	BV8	QQGGTEA	1.1	0.01572
		clono 11	BV8	SLGGTEA	1.1	0.01975
		clono 12	BV13	RTGLDGY	1.2	0.03094
		clono 13	BV13	SYVGGKAEA	1.2	0.02612
A2/CMV-pp65	BCL4	clono 1	BV1	SVYGGAGNSPL	1.6	0.00866
		clono 2	BV1	SYPGGNTI	1.3	0.01797
		clono 3	BV3	SFLGYTEA	1.1	0.01174
		clono 4	BV8	SSVNEA	1.1	0.00646
		clono 5	BV8	SSAGGAVYGY	1.2	0.02039
		clono 6	BV9	SLLLGTAAEA	1.1	0.00313
		clono 7	BV14	RLLAGGRSAQ	2.5	0.00608
		clono 8	BV3	SFSSPGQGSTDQ	2.3	0.01285
		clono 9	BV8	SSVLEA	1.1	0.01002
		clono 10	BV8	SLVGGVDGY	1.2	0.03013
		clono 11	BV8	SIMDYGY	1.2	0.03125
		clono 12	BV13	SAVTGAVDQPQ	1.5	0.01642
		clono 13	BV13	SYFYEQ	2.7	0.00251
		clono 14	BV13	SYSTGTAYGY	1.2	0.00289
		clono 15	BV13	SPKTGVPYEQ	2.7	0.02146
	BCL6	clono 16	BV8	SSANYGY	1.2	0.01505
		clono 17	BV13	SRQTGAAYGY	1.2	0.00617
		clono 18	BV13	SYATGTAYGY	1.2	0.00530
A2/EBV-BMFL1	BCL4	clono 1	BV2	RDRTGNGY	1.2	0.005131
		clono 2	BV2	RDSVGNNGY	1.2	0.002706
		clono 3	BV2	RDRVGNNGY	1.2	0.001934
		clono 4	BV2	RDSTGNGY	1.2	0.004689
		clono 5	BV2	RVEPGNGY	1.2	0.009871
		clono 6	BV4	VGTGGTNEKL	1.4	0.014417
		clono 7	BV4	VGYGGTNEKL	1.4	0.013503
		clono 8	BV4	VGSGGTNEKL	1.4	0.045620
		clono 9	BV16	SQSPGGTQ	2.5	0.009123
		clono 10	BV16	SQSPGGEA	1.1	0.003469
		clono 11	BV16	SQSPGGTS	na	0.003878
		clono 12	BV18	SPPAVSYEQ	2.7	0.016529
		clono 13	BV2	DGY	1.2	0.017560

Supplemental Table 2. List of antibodies used in this study.

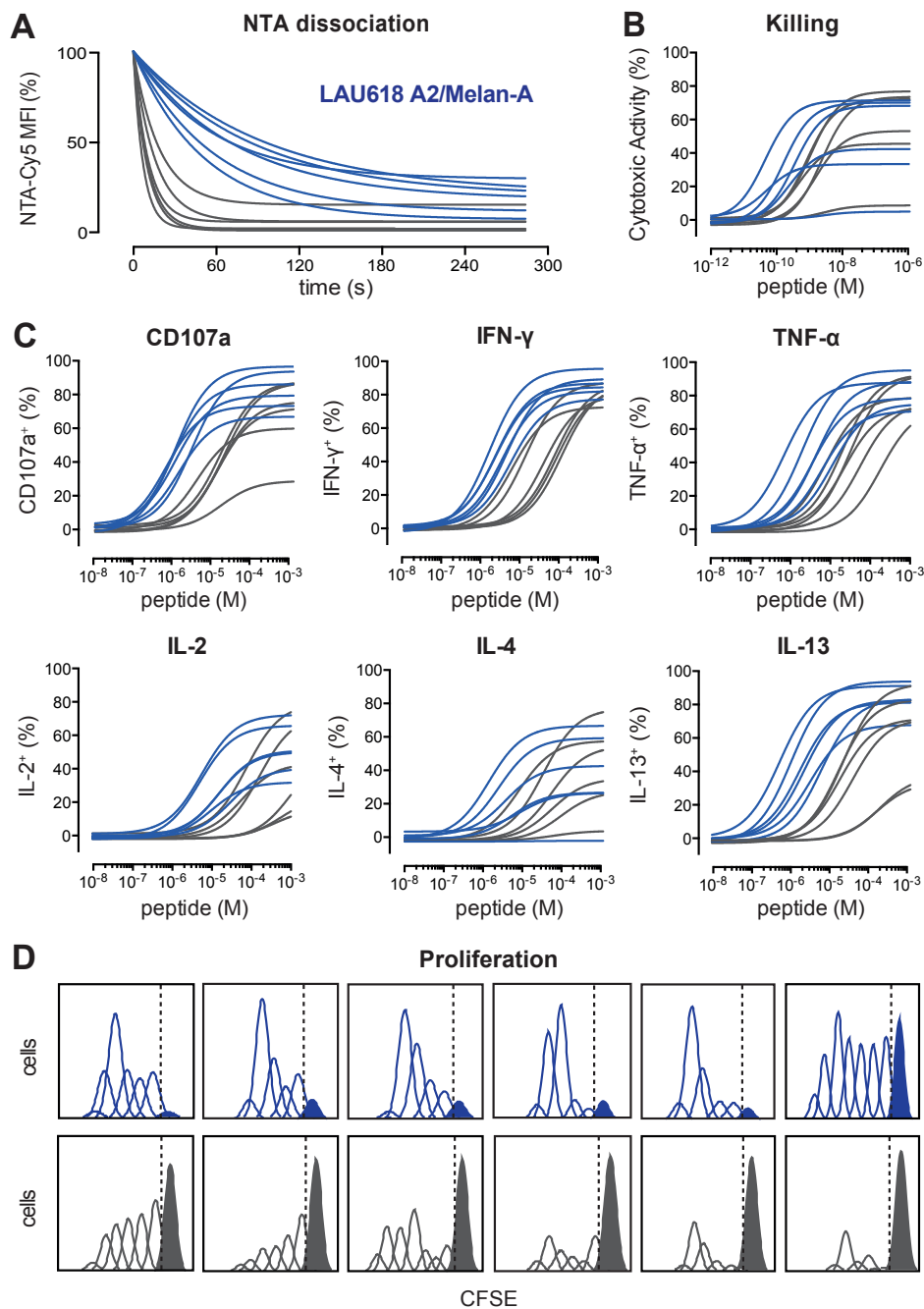
Name	Company	Catalog no	Clone no
APC anti-CD28	BD Pharmigen	559770	CD28.2
FITC anti-CD45RA	BD Pharmigen	561882	HI100
FITC anti-CD107a	BD Pharmigen	555800	H4A3
PerCPCy5.5 anti-IL2	BD Pharmigen	560708	MQ1-17H12
APC anti-IL13	BD Pharmigen	561162	JES10-5A2
PE-Cy7 anti-IFN γ	BD Pharmigen	557844	4S.B3
A700 anti-TNF α	BD Pharmigen	557996	MAb11
PE-Cy7 anti-CD5	BD Pharmigen	348810	L17F12
APC anti-CD137	BD Pharmigen	550890	4B4-1
PE anti-VLA-1	BD Pharmigen	559596	SR84
APC anti-VLA-4	BD Pharmigen	561794	MAR4 .
BrV421 anti-PD1	BD Pharmigen	562516	EH12.1
APC-A750 anti-CD8	Beckman Coulter	A94683	B9.11
Pacific-blue anti-CD8	Beckman Coulter	A82791	B9.11
FITC anti-CD8beta	Beckman Coulter	IM2217U	2ST8.5H7
PE-Cy7 anti-CD8alpha	Beckman Coulter	737661	SFCI21Thy2D3
PE anti-pan-TCRab	Beckman Coulter	A39499	IP26A
PE-Cy7 anti-CCR7	Biolegend	353226	G043H7
PE anti-IL4	Biolegend	500810	MP4-25D2
BrV421 anti-CD28	Biolegend	302930	CD28.2
A488 anti-PD1	AbD Serotech	MCA2628A488	MIH4
APC anti-TIGIT	eBioscience	17-9500-42	MBSA43
FITC anti-LAG-3	Enzo	ALX-804-806F-C100	17B4
PE anti-TIM-3	R&D systems	FAB2365P	344823



Sup Figure 1 - Allard et al.

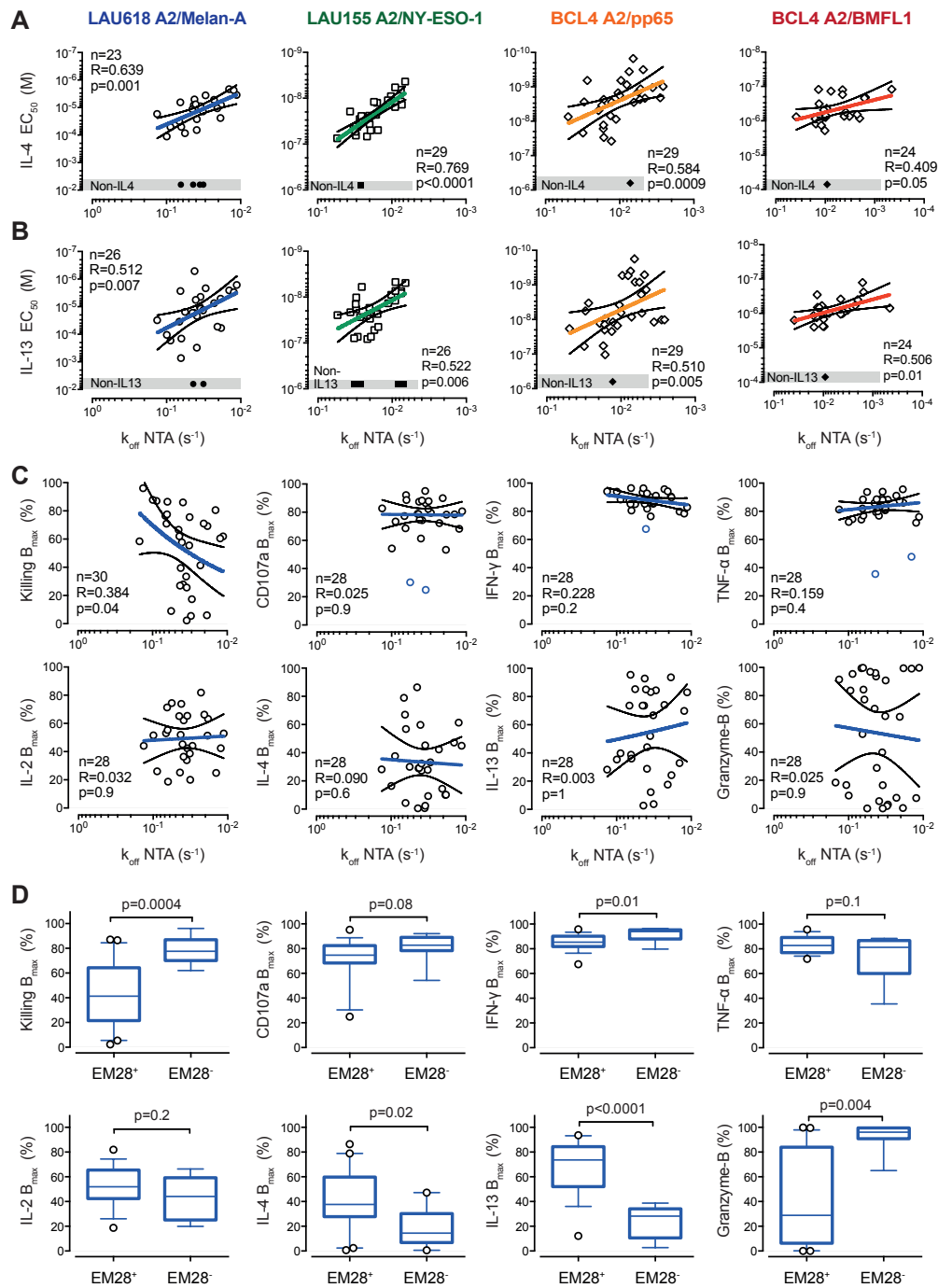
Supplemental Figure 1: Ex vivo detection of antigen-specific CD8 T cells using pMHC-based reagents and analysis of blood samples used to generate self/tumor- and virus-specific CD8 T cell clones. (A) Comparison of A2/MelanA₂₆₋₃₅-specific staining from PBMCs obtained from melanoma patients (LAU1129 and LAU1164) using PE-labeled pentamers, streptamers, multimers and NTAMers. Gating was done on live CD14⁻/CD16⁻/CD19⁻/CD3⁺ lymphocytes. The valence of pMHC reagents is indicated in brackets, as well as percentages of positively stained cells. FMO (fluorescence minus one). **(B)** CD8 and multimer staining of CD8-enriched PBMCs from melanoma patients LAU618 (A2/Melan-A₂₆₋₃₅), LAU155 (A2/NY-ESO-1₁₅₇₋₁₆₅) and healthy donor BCL4 (A2/pp65₄₉₅₋₅₀₄ or A2/BMFL1₁₂₅₉₋₂₆₇). **(C)** CCR7, CD45RA and CD28 staining of the corresponding multimer-

specific (*RI*) and total CD8 T cell (*CD8t*) populations. Percentages of positively stained cells are indicated. Melan-A-specific CD8 T cell clones (from patient LAU618) exhibited an EM/CD28^{+/-} phenotype, while NY-ESO-1-specific T cell clones (from patient LAU155) presented mostly an early-differentiated EM/CD28⁺ phenotype. EBV/BMFL1-specific CD8 T cell clones were predominantly EM/CD28⁺, whereas CMV/pp65-specific clones mostly exhibited a differentiated EMRA/CD28⁻ phenotype.



Sup Figure 2 - Allard et al.

Supplemental Figure 2: *In vitro* analysis of TCR dissociation-rates versus functional avidities of self/tumor- and virus-specific CD8 T cell clones. Representative (A) NTAmers-dissociation curves, (B) killing-, (C) CD107a degranulation-, IFN γ -, TNF α -, IL-2-, IL-4- and IL-13-production titration curves and (D) proliferation analysis (by CFSE fluorescence histograms) obtained for A2/Melan-A₂₆₋₃₅-specific CD8 T cell clones from patient LAU618, defined as slow (n = 6, blue lines) or fast (n = 6, grey lines) TCR off-rates. Non-divided and divided T cells are represented as plain and empty peaks, respectively.

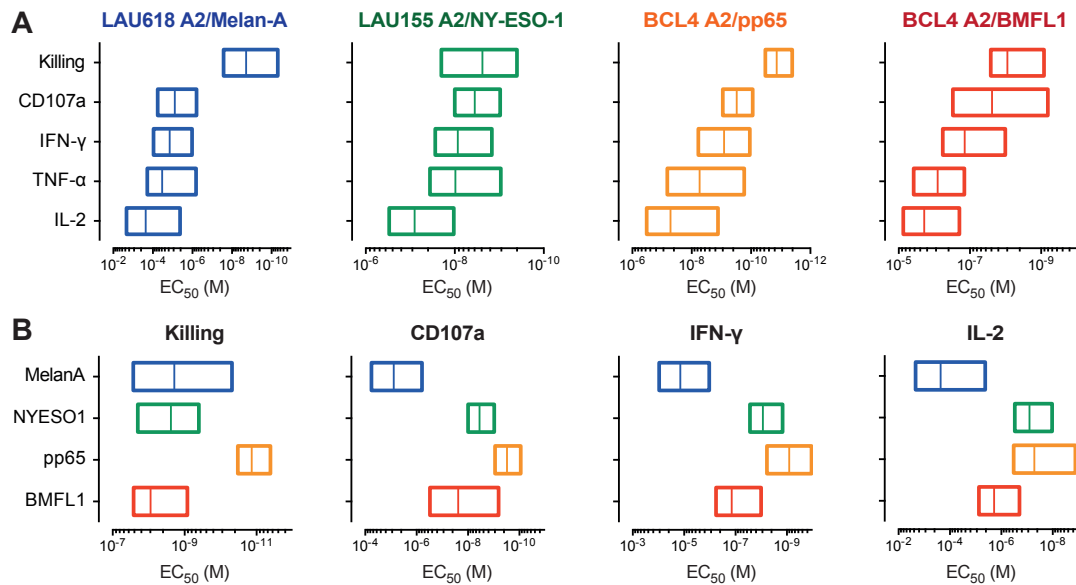


Sup Figure 3 - Allard et al.

Supplemental Figure 3: Relationship between TCR dissociation-rates, functional avidity and maximal function capacity of self/tumor- and virus-specific CD8 T cell clones.

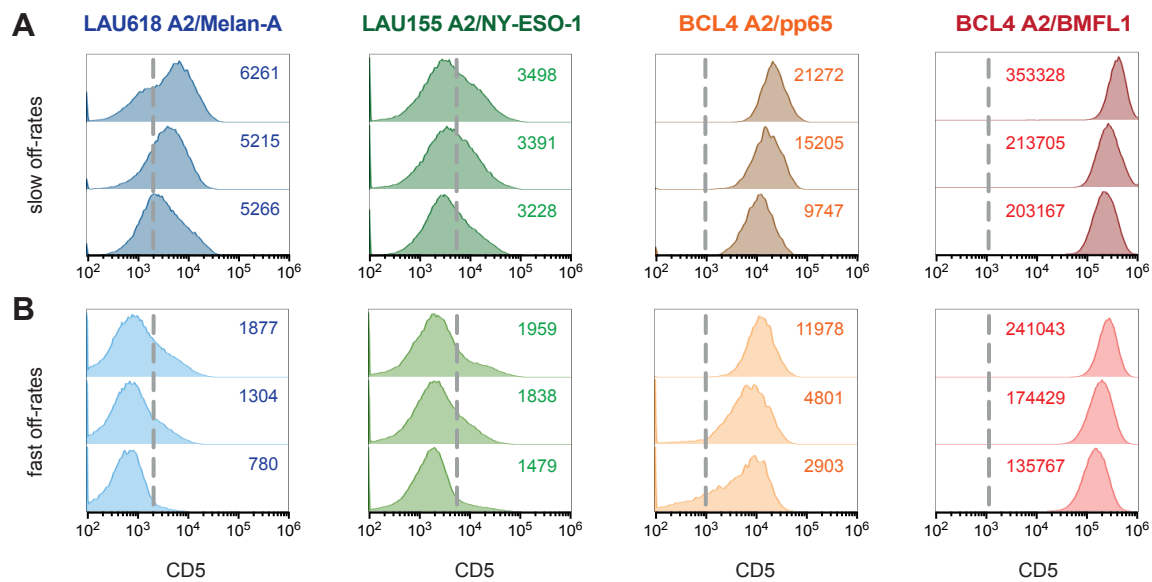
Correlations between EC_{50} values from (A) IL-4- and (B) IL-13-production titration assays, and NTamer-derived TCR dissociation-rates (k_{off}). (C) Correlations between B_{max} values from killing, CD107a-degranulation, $IFN\gamma$ -, $TNF\alpha$ -, IL-2-, IL-4- and IL-13-production titration assays, or percentages of granzyme-B expressing T cells, and NTamer-derived TCR dissociation-rates (k_{off}). (A-C) Each data-point represents an A2/Melan-A₂₆₋₃₅- (derived from patient LAU618, ○), A2/NY-ESO-1₁₅₇₋₁₆₅- (patient LAU155, □), A2/pp65₄₉₅₋₅₀₄- or

A2/BMFL1₂₅₉₋₂₆₇- (healthy donor BCL4, \diamond) specific individual T cell clone. Non-functional clones are represented in grey boxes. The number of clones displaying function n , as well as Spearman's correlation (two tailed, $\alpha = 0.05$) coefficient R and p values are indicated. Color-coded and black lines are indicative of regression fitting and 95% confidence intervals, respectively. **(D)** B_{\max} values from killing, CD107a-degranulation, IFN γ -, TNF α -, IL-2-, IL-4- and IL-13-production titration assays, or granzyme-B expression, of early-differentiated effector-memory EM/CD28⁺ or late-differentiated EM/CD28⁻ A2/Melan-A₂₆₋₃₅-specific T cell clones derived from patient LAU618. Data are depicted as box (25th to 75th percentiles) and whisker (10th to 90th percentiles) with the middle line representing the median. Numbers of clones n , as well as Mann-Whitney (two tailed) derived p values are indicated. Of note, upon high peptide-dose stimulation (at B_{\max} , maximal response), differentiated EM/CD28⁻-derived CD8 T cell clones displayed higher granzyme-B expression, cytotoxic and IFN- γ production capacity, but a lower ability to produce IL-2, IL-4 or IL-13 than memory EM/CD28⁺ T cells.



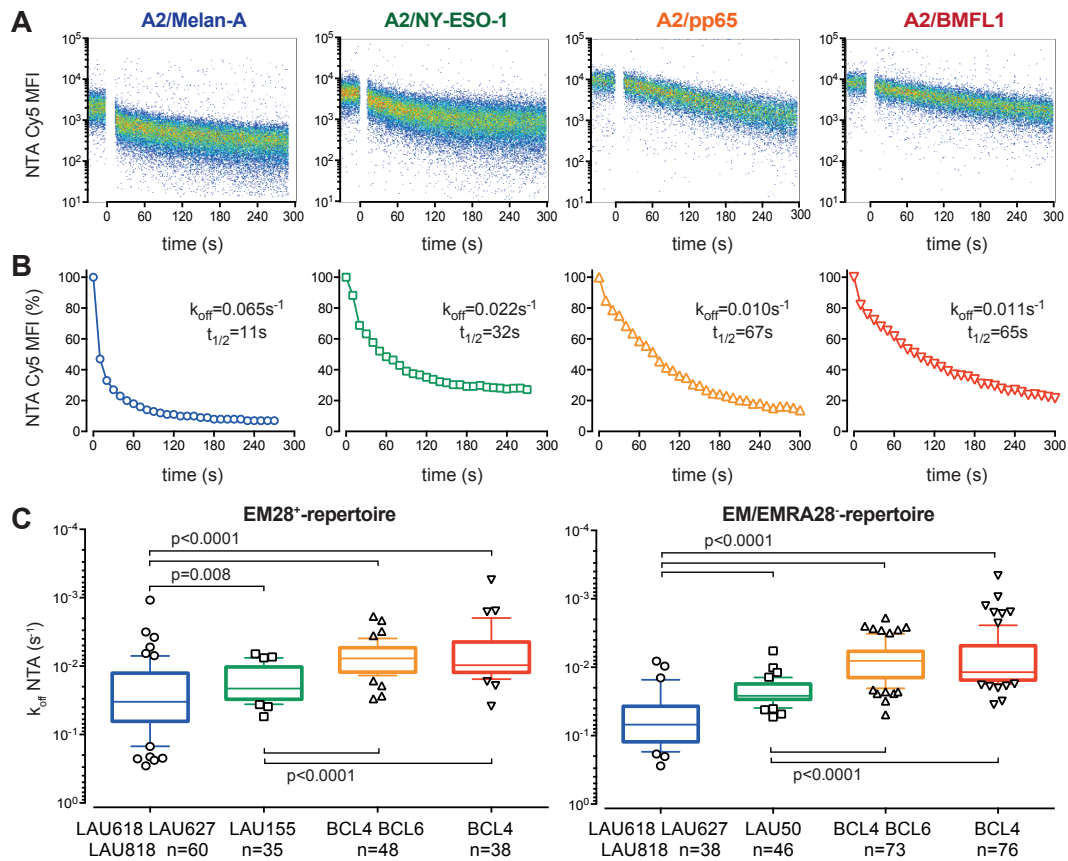
Sup Figure 4 - Allard et al.

Supplemental Figure 4: Functional avidities according to the functional assay or the antigenic specificity of CD8 T cell clones. Comparison of functional avidity (EC_{50}) from killing-, CD107a degranulation-, IFN γ -, TNF α - and IL-2-production of A2/Melan-A₂₆₋₃₅- (derived from melanoma patient LAU618, n = 30), A2/NY-ESO-1₁₅₇₋₁₆₅- (patient LAU155, n = 32), A2/pp65₄₉₅₋₅₀₄- or A2/BMFL1₂₅₉₋₂₆₇- (healthy donor BCL4, n = 30 and 26, respectively) specific CD8 T cell clones classified according to (A) the functional assay and (B) the antigenic-specificity. Data are depicted as box (minimum to maximum) with the middle line representing the mean. The representative TCR-BV clonotype diversity of each antigenic specificity is as following; LAU618/Melan-A, 77%; LAU155/NY-ESO-1, 43%; BCL4/pp65, 57%; BCL4/BMFL1, 67%.



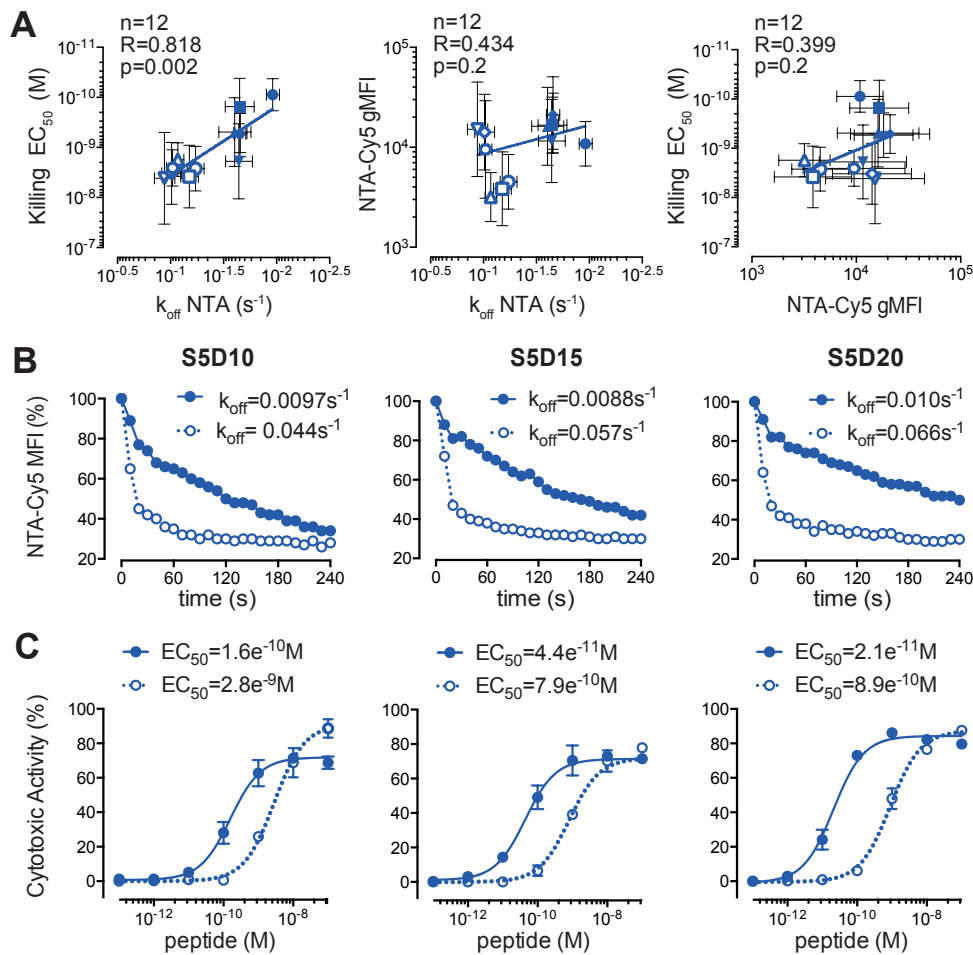
Sup Figure 5 - Allard et al.

Supplemental Figure 5: CD5 expression according to the TCR-dissociation off-rate parameter and antigenic specificity of self/tumor- and virus-specific CD8 T cell clones. CD5 surface staining was obtained at baseline (no antigen-specific stimulation) from representative antigen-specific CD8 T cells of (A) slow or (B) fast NTAmer-based off-rates. Data are depicted according to the antigenic specificity (A2/Melan-A₂₆₋₃₅-, A2/NY-ESO-1₁₅₇₋₁₆₅-, A2/pp65₄₉₅₋₅₀₄- and A2/BMFL1₂₅₉₋₂₆₇ antigens). Geometric fluorescence means (gMFI) are indicated.



Sup Figure 6 - Allard et al.

Supplemental Figure 6: TCR dissociation-rates according to the antigenic specificity and *ex vivo* differentiation status. Representative (A) NTamer-dissociation staining and (B) corresponding fitting curve obtained for A2/Melan-A₂₆₋₃₅- (○), A2/NY-ESO-1₁₅₇₋₁₆₅- (□), A2/pp65₄₉₅₋₅₀₄- (△) and A2/BMFL1₂₅₉₋₂₆₇- (▽) specific CD8 T cell clones, defined as average TCR off-rates. k_{off} and $t_{1/2}$ derived values are indicated. (C) NTamer-derived TCR dissociation-rates (k_{off}) of early-differentiated effector-memory EM CD28⁺ (left panel) versus late-differentiated EM/EMRA CD28⁻ (right panel) clones specific for (i) A2/Melan-A₂₆₋₃₅ (from vaccinated melanoma patients LAU618, LAU627 and LAU818), (ii) A2/NY-ESO-1₁₅₇₋₁₆₅ (from patients LAU50 and LAU155 with naturally occurring tumor-specific T cell responses) or (iii) the persistent herpes viruses A2/pp65₄₉₅₋₅₀₄ or A2/BMFL1₂₅₉₋₂₆₇ (from healthy donors BCL4 and BCL6), categorized according to their antigenic specificity. Data are depicted as box (25th to 75th percentiles) and whisker (10th to 90th percentiles), with the middle line representing the median. Antigen specificity is depicted according to specific colored codes and symbols. Numbers of clones n , as well as Kruskal-Wallis test ($\alpha = 0.05$) derived p values are indicated. Significant differences between the A2/Melan-A₂₆₋₃₅- and the A2/NY-ESO-1₁₅₇₋₁₆₅-specific groups were obtained by a Mann Whitney test (two tailed).



Sup Figure 7 - Allard et al.

Supplemental Figure 7: Correlations between TCR dissociation rates versus pMHC multimer staining versus functional avidity of CD8 T cell clones. (A) Correlations between NTamer-derived TCR dissociation rates (k_{off}), NTamer surface staining levels (gMFI) and killing avidity values (EC_{50}) obtained from independent assays ($n = 4$ to 9) for A2/Melan-A₂₆₋₃₅-specific CD8 T cell clones, defined as slow ($n = 6$, plain symbols) or fast ($n = 6$, empty symbols) TCR off-rates. Each symbol/clone is represented as average \pm SD. The number of clones (n), as well as Spearman's correlation (two tailed, $\alpha = 0.05$) coefficients R and p values are indicated. Lines are indicative of linear regression fitting. Representative (B) NTamer-dissociation and (C) killing-titration curves obtained at day 10 (D10), 15 (D15) and 20 (D20) following non-specific stimulation (by PHA and irradiated feeder cells) of A2/Melan-A₂₆₋₃₅-specific CD8 T cell clones, defined as slow ($n = 6$, plain symbols and solid lines) or fast ($n = 6$, empty symbols and dotted lines) TCR off-rates. Average and SD percentages are depicted, as well as the corresponding fitting curves and k_{off} or EC_{50} derived values.